Amino Acids of the *Torpedo marmorata* Acetylcholine Receptor α Subunit Labeled by a Photoaffinity Ligand for the Acetylcholine Binding Site†

Michael Dennis,‡,§ Jérôme Giraudat,‡ Florence Kotzyba-Hibert,‖ Maurice Goeldner,‖ Christian Hirth,‖ Jui-Yoa Chang,⊥ Claude Lazure,# Michel Chrétien,# and Jean-Pierre Changeux*,‡

Neurobiologie Moléculaire et Laboratoire Associé au CNRS (UA 041149), Interactions Moléculaires et Cellulaires, Institut Pasteur, 25 Rue du Dr. Roux, 75724 Paris Cédex 15, France, Laboratoire de Chimie Bioorganique, Laboratoire Associé au CNRS (UA 31), Faculté de Pharmacie, Université Louis Pasteur, 74 Route du Rhin, 67400 Illkirch, France, Pharmaceutical Research Laboratories, Ciba-Geigy Ltd., CH-4002 Basel, Switzerland, and Laboratoire d'Endocrinologie Moléculaire, Institut de Recherches Cliniques de Montréal, 110 Avenue des Pins Ouest, Montreal, Canada H2W 1R7

Received August 27, 1987; Revised Manuscript Received November 10, 1987

ABSTRACT: The acetylcholine-binding sites on the native, membrane-bound acetylcholine receptor from *Torpedo marmorata* were covalently labeled with the photoaffinity reagent [^{3}H]-*p*-(dimethylamino)-benzenediazonium fluoroborate (DDF) in the presence of phencyclidine by employing an energy-transfer photolysis procedure. The α-chains isolated from receptor-rich membranes photolabeled in the absence or presence of carbamoylcholine were cleaved with CNBr and the radiolabeled fragments purified by high-performance liquid chromatography. Amino acid and/or sequence analysis demonstrated that the α-chain residues Trp-149, Tyr-190, Cys-192, and Cys-193 and an unidentified residue(s) in the segment α 31–105 were all labeled by the photoaffinity reagent in an agonist-protectable manner. The labeled amino acids are located within three distinct regions of the large amino-terminal hydrophilic domain of the α-subunit primary structure and plausibly lie in proximity to one another at the level of the acetylcholine-binding sites in the native receptor. These findings are in accord with models proposed for the transmembrane topology of the α-chain that assign the amino-terminal segment α 1–210 to the synaptic cleft. Furthermore, the results suggest that the four identified [^{3}H]DDF-labeled residues, which are conserved in muscle and neuronal α-chains but not in the other subunits, may be directly involved in agonist binding.

The nicotinic acetylcholine receptor (AcChoR)[1] from vertebrate muscle and fish electric organ is a pentamer of four different but homologous polypeptides in the stoichiometry $\alpha_2\beta\gamma\delta$ which both carries the acetylcholine (AcCho) binding sites and contains the cation-selective channel-forming elements [reviewed by Popot and Changeux (1984), Wennogle (1986), McCarthy et al. (1986), and Hucho (1986)]. Nicotinic agonists, competitive antagonists, and snake venom α-toxins bind reversibly and in a mutually exclusive manner to a class of "primary" AcCho-binding sites present in two copies per receptor oligomer (Neubig & Cohen 1979, 1980). Covalent labeling of these sites on the reduced AcChoR with sulfhydryl-directed affinity reagents invariably leads to exclusive labeling of the α-chains [reviewed by Karlin (1983)], indicating that each of the two α-subunits carries all or part of an AcCho-binding site. This interpretation is supported by studies showing that the α-subunit alone, either isolated from AcChoR-rich membranes (Haggerty & Froehner, 1981; Tzartos & Changeux, 1983, 1984; Gershoni et al., 1983) or expressed in frog oocytes from the corresponding cDNA (Mishina et al., 1984), exhibits α-toxin-binding capacity, whereas the other AcChoR chains do not.

In an attempt to identify the region(s) of the α-chain primary structure forming the AcCho-binding sites, Kao et al. (1984) showed that the α-subunit residues Cys-192 and -193 are labeled by the sulfhydryl-directed affinity reagent 4-(*N*-maleimido)benzyltrimethylammonium iodide, suggesting that the corresponding sulfhydryl groups lie within 1 nm of the AcCho-binding site on the reduced AcChoR (Karlin, 1969). It has been shown, however, that reduction markedly alters the affinity and selectivity of the AcChoR for cholinergic ligands (Karlin, 1969; Walker et al., 1984). An alternative approach employed by several groups involves the analysis of α-toxin binding to α-chain proteolytic fragments (Wilson et al., 1984, 1985; Neumann et al., 1985, 1986a), synthetic peptides (Wilson et al., 1985; Mulac-Jericevic & Atassi, 1986; Neumann et al., 1986b; Ralston et al., 1987), and deletion mutants (Barkas et al., 1987). The results of such studies, while carried out with preparations that bind α-toxin with affinities several orders of magnitude lower than native AcChoR and in an agonist-insensitive manner [see, however, Neumann et al. (1986b)], also point to the region containing Cys-192 and -193 as a potential site of interaction with cholinergic ligands. Finally, it has been reported that a 20-kDa proteolytic fragment of the α-chain extending from α Ser-173, and thus containing Cys-192 and -193, carries the site of photoincorporation of [^{3}H]-*d*-tubocurarine (Pedersen et al., 1986).

In order to probe the structure of the AcCho-binding sites on the native AcChoR in greater detail, we have employed a

† This work was supported by the Muscular Dystrophy Association of America, the Collège de France, the Ministère de la Recherche et de l'Enseignement Supérieur, the Centre National de la Recherche Scientifique, the Commissariat à l'Energie Atomique, and the Medical Research Council of Canada (Grant PG-2). M.D. was supported by a fellowship from the Fonds de la Recherche en Santé du Québec.

‡ Institut Pasteur.

§ Present address: Protein Engineering Group, Biotechnology Research Institute, 6100 Royalmount Ave., Montreal, Canada H4P 2R2.

‖ Université Louis Pasteur.

⊥ Ciba-Geigy Ltd.

Institut de Recherches Cliniques de Montréal.

[1] Abbreviations: AcChoR, acetylcholine receptor; AcCho, acetylcholine; DDF, *p*-(dimethylamino)benzenediazonium fluoroborate; α-BgTx, α-bungarotoxin; $NaDodSO_4$, sodium dodecyl sulfate; HPLC, high-performance liquid chromatography; PTH amino acids, phenylthiohydantoin amino acids; kDa, kilodaltons.

0006-2960/88/0427-2346$01.50/0

photoaffinity ligand for these sites, the aryldiazonium derivative *p*-(dimethylamino)benzenediazonium fluoroborate (DDF), which gives rise upon photolysis to an extremely reactive aryl cation moiety. As shown in the accompanying paper (Langenbuch-Cachat et al., 1988), DDF acts as a reversible competitive antagonist for the AcCho-binding sites in the dark and irreversibly blocks these sites on native, unreduced AcChoR following irradiation, with cholinergic agonists and competitive antagonists preventing this inactivation. In the presence of phencyclidine, to protect the high-affinity site for noncompetitive blockers and by employment of energy transfer from Trp residues of the AcChoR protein to photoactivate bound ligand preferentially, the incorporation of [^{3}H]DDF into native AcChoR from *T. marmorata* is markedly inhibited by cholinergic ligands and exhibits a stoichiometry of approximately one molecule of [^{3}H]DDF incorporated in an agonist-protectable manner per inactivated α-bungarotoxin (α-BgTx) binding site. Under these conditions, [^{3}H]DDF labels predominantly the AcChoR α-chain.

We have previously reported (Dennis et al., 1986) that the major target of carbamoylcholine-protectable labeling of the α-subunit with [^{3}H]DDF corresponds to the fragment α 179–207. In the present study, we have identified several amino acids within this fragment that are photolabeled by [^{3}H]DDF in an agonist-protectable manner. The results further demonstrate additional sites of carbamoylcholine-protectable labeling located in two distinct regions of the α-chain primary structure. These findings provide information on the tertiary folding of the α-subunit at the level of the cholinergic binding sites and suggest that multiple regions of the α-chain may participate in AcCho binding in the native AcChoR.

Materials and Methods

[^{3}H]DDF (0.75 Ci/mmol) was prepared as described in the accompanying paper (Langenbuch-Cachat et al., 1988). Phencyclidine was generously provided by A. Jaganathen (Université Louis Pasteur, Strasbourg, France). Carbamoylcholine was purchased from Sigma and CNBr from Eastman Kodak. Live *T. marmorata* were obtained from the Biological Station of Arcachon (France).

Covalent Labeling of the AcChoR by [^{3}H]DDF. Preparative photolabeling of large batches (100–200 nmol of α-BgTx-binding sites) of purified (Saitoh et al., 1980) and alkali-treated (Neubig et al., 1979) AcChoR-rich membrane fragments was achieved by energy transfer (λ = 290 nm) as described in the accompanying paper (Langenbuch-Cachat et al., 1988), except that the total volume for each irradiation was 2.0 mL. Final concentrations during irradiation were 1–2 μM α-BgTx-binding sites at approximately 1 nmol of sites/mg of protein, 100 μM phencyclidine, 200 μM [^{3}H]DDF and, when indicated, 100 μM carbamoylcholine.

Following irradiation, dithiothreitol was added to a final concentration of 10 mM to destroy unreacted [^{3}H]DDF, and aliquots of the membrane suspensions were removed for titration of α-BgTx-binding sites (Weber & Changeux, 1974); the remainder was centrifuged and the pellets solubilized in $NaDodSO_4$ sample buffer (Laemmli, 1970). Aliquots of the solubilized membranes were analyzed on $NaDodSO_4$–polyacrylamide gels, and the incorporation of radioactivity into the various AcChoR subunits was quantified as previously described (Dennis et al., 1986). The amount of each polypeptide was quantified by densitometric scanning of the Coomassie blue stained gel using bovine serum albumin as standard.

Purification of the α-Chain. Solubilized membranes were subjected to preparative $NaDodSO_4$–polyacrylamide gel electrophoresis and the separated AcChoR subunits eluted by diffusion (Giraudat et al., 1986). The eluates were dialyzed against 0.1% $NaDodSO_4$/0.01% thioglycol and then against water and lyophilized. The purified α-chain was carboxymethylated and then precipitated twice with acetone (Giraudat et al., 1986).

The purified α-chain migrated as a single band on a polyacrylamide gel, and its specific radioactivity was not significantly different from that estimated just after irradiation (15 000 dpm/μg of α-chain vs 4300 dpm/μg of α-chain for the carbamoylcholine-protected batch). The recovery of the α-chain following purification was approximately 50%.

Cleavage of the α-Chain. The purified, carboxymethylated α-chain was dissolved in 70% formic acid (2 mg of protein/mL) and Trp added in a 5-fold molar excess (4 mM) over Met residues to protect against oxidation of endogenous Trp. CNBr was then added to a final concentration of 0.06 M (100-fold excess over Met), and the mixtures were incubated for 24 h at room temperature under nitrogen in the dark. The samples were then diluted with 3 volumes of water and lyophilized.

Purification of Peptides. Dried CNBr digests were resuspended in 4 M guanidine hydrochloride in 0.1% trifluoroacetic acid/6% 1-propanol/3% acetonitrile in H_2O. Following centrifugation, the supernatants were transferred, the pellets reextracted twice with the same solvent, and the supernatants pooled. The final pellets were dissolved in pure formic acid and diluted with 5–10 volumes of 0.1% trifluoroacetic acid/6% 1-propanol/3% acetonitrile in H_2O. The supernatant and pellet fractions prepared as described above were subjected separately to reversed-phase high-performance liquid chromatography (HPLC) on a Brownlee RP-300 Aquapore column (4.6 × 250 mm) and selected peaks of radiolabeled material repurified on the same column as detailed in the figure legends. Gel permeation HPLC of repurified peptides was performed by using Bio-Rad TSK columns (type 125 and 250) connected in series (see figure legends). Dried samples were dissolved in deionized 8 M urea in 10% acetic acid for injection (total volume $\leq$200 μL) and the columns eluted with the same solvent at a flow rate of 0.5 mL/min. The HPLC system used was as described (Dennis et al., 1986).

Sequence Analyses. Automated Edman degradation was carried out on an Applied Biosystems gas-phase automated sequenator. Peptides were dissolved in 50% formic acid or 50% trifluoroacetic acid for loading. Aliquots of the sequenator output were used for identification and quantification of phenylthiohydantoin (PTH) amino acids by HPLC (Knecht et al., 1983; Lazure et al., 1983) and for radioactivity measurements by liquid scintillation counting.

Amino acid analyses were performed by using a Beckman Model 7300 analyzer. Hydrolyses were carried out in the vapor phase under reduced pressure by exposing dried samples to 6 N HCl containing β-mercaptoethanol for 24 h at 110 °C (Dabre, 1986).

Results

Labeling of the α-Chain by [^{3}H]DDF. Alkali-treated AcChoR-rich membrane fragments were photolabeled with [^{3}H]DDF in the presence of 100 μM phencyclidine according to energy-transfer irradiation procedure described in the accompanying paper (Langenbuch-Cachat et al., 1988), leading to an irreversible loss of 30–35% of the available α-BgTx-binding sites. The α-chain, which carried the majority (approximately 75%) of the [^{3}H]DDF associated with the AcChoR polypeptides, was purified. From the specific activity

of the [^{3}H]DDF employed, the extent of carbamoylcholine-protectable labeling of the purified material was estimated as 0.32 mol of DDF/mol of α-chain (0.45 mol of DDF/mol of α-chain for the unprotected batch vs 0.13 mol of DDF/mol of α-chain for the carbamoylcholine-protected batch).

Fractionation of α-Chain CNBr Digests. Equal amounts (approximately 0.75 mg) of α-chain isolated from membranes labeled in the absence and presence of carbamoylcholine were carboxymethylated and treated with CNBr in parallel. Extraction of the dried CNBr digests with 4 M guanidine hydrochloride in low concentrations of organic solvent (see Materials and Methods) solubilized 70–75% of the radioactivity for the α-chain from unprotected membranes and 25–30% of the radioactivity for the α-chain from carbamoylcholine-protected membranes. In both cases, the radioactivity remaining in the pellet could be completely solubilized in pure formic acid.

Analysis of the material soluble in guanidine hydrochloride containing medium by reversed-phase HPLC yielded the chromatograms shown in Figure 1. The UV_{210} absorbance profiles for the unprotected (A) and carbamoylcholine-protected (B) samples were qualitatively and quantitatively very similar, indicating that the same polypeptides had been solubilized from both samples. Approximately 3–5% of the injected radioactivity was associated with unbound material in both analyses, the absolute amount of radioactivity in this fraction being only slightly decreased in the carbamoylcholine-protected sample; this material was not further analyzed. The unprotected sample exhibited three additional peaks of radioactivity eluting between 23 and 27% (I), 28 and 34% (II), and 41 and 42% (III) solvent B; the radioactivity associated with all three of these peaks was markedly reduced (by 75–85%) in the carbamoylcholine-protected sample. These three radioactive peaks, which together accounted for approximately 70% of the total agonist-protectable labeling of the α-chain, were thus selected for further characterization.

Approximately 5% of the radioactive material soluble in guanidine hydrochloride containing medium eluted at 100% solvent B upon reversed-phase HPLC analysis, but radioactivity associated with this hydrophobic material was only moderately decreased (by approximately 40%) in the carbamoylcholine-protected sample (data no shown). When the radioactive material remaining in CNBr digests following extraction with guanidine hydrochloride containing medium was solubilized in formic acid and analyzed by reversed-phase HPLC, essentially all of the radioactivity was associated with this highly hydrophobic fraction and showed only modest reduction in the carbamoylcholine-protected material (data not shown). This hydrophobic material, which accounted for the vast majority of the agonist-insensitive labeling of the α-chain, was not further characterized.

Characterization of [^{3}H]DDF-Labeled Material in Peak I. As shown in Figure 1A, the radioactivity present in peak I, which represented approximately 5% of the total agonist-protectable labeling of the α-subunit, comprised a sharply rising peak of tritium (fractions 28–29) plus a shoulder on the descending portion (fractions 31–33). Radioactivity associated with each component was decreased by approximately 85% in the carbamoylcholine-protected sample (Figure 1B).

Fractions corresponding to the sharply rising portion of the peak of radioactivity contained multiple UV_{210} absorbing species. Sequence analysis of an aliquot of the pool of fractions (Ia in Figure 1A) revealed two amino-terminal sequences (data not shown), a minor one (Lys-Leu-Gly...), corresponding to a CNBr fragment of the α-chain extending from αLys-145,

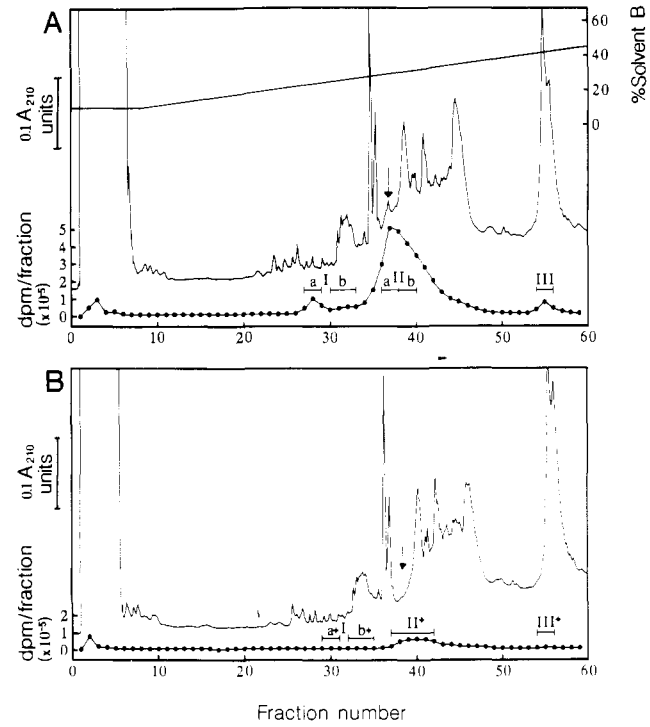

FIGURE 1: Reversed-phase HPLC of CNBr digests of the [^{3}H]-DDF-labeled α-chain. The α-subunits (approximately 0.75 mg) isolated from AcChoR-rich membranes photolabeled with [^{3}H]DDF in the absence (A) or presence (B) of 100 μM carbamoylcholine were carboxymethylated and cleaved with CNBr. The dried digests were extracted with 4 M guanidine hydrochloride containing medium (see Materials and Methods), and half of the soluble material was injected onto a Brownlee RP-300 reversed-phase column equilibrated in 90% solvent A (0.1% trifluoroacetic acid)/10% solvent B (0.1% trifluoroacetic acid, 60% 1-propanol, 30% acetonitrile). The column was eluted at a flow rate of 1.0 mL/min with the gradient of solvent B indicated in (A) and the UV absorbance of the eluates was monitored at 210 nm (solid trace); as a result of uncontrolled variability between HPLC runs, the corresponding UV absorbing peaks eluted approximately 4 min later in (B) as compared to in (A). Aliquots (20 μL) of 2.0-mL fractions were taken for radioactivity measurements (●); data points are plotted at the end of the time period for the corresponding fraction. The recoveries of injected radioactivity in (A) and (B) were 78 and 76%, respectively. Material contained in pools of fractions denoted by horizontal bars was either repurified or subjected directly to sequence analysis (see text). Roman numerals designate peaks of radioactivity decreased in the carbamoylcholine-protected sample. The arrows indicate the elution position of a highly radioactive UV absorbing component specific to the material labeled in the absence of carbamoylcholine.

plus a major sequence that could not be aligned within the known primary structures of *T. marmorata* α-chain (Devillers-Thiéry et al., 1983) or of the other AcChoR polypeptides from *T. californica* (Noda et al., 1983). Material in pool Ia was thus rechromatographed on the same column using heptafluorobutyric acid as counterion (see legend to Figure 2). The single peak of tritium observed in this analysis (data not shown), which accounted for approximately 70% of the injected radioactivity, was reanalyzed by using trifluoroacetic acid as counterion, yielding a nonsymmetrical peak of UV_{210} absorbing material that coeluted with the peak of radioactivity (Figure 2A). The corresponding fractions (23–25) were pooled (pool Ia1), and an aliquot was subjected to gel permeation HPLC. As shown in Figure 2B, a single radiolabeled component was observed that exhibited an apparent molecular weight of approximately 4200.

Sequence analysis of the repurified species in pool Ia1 revealed a single amino-terminal sequence corresponding to the unique α-chain CNBr fragment extending from Lys-145

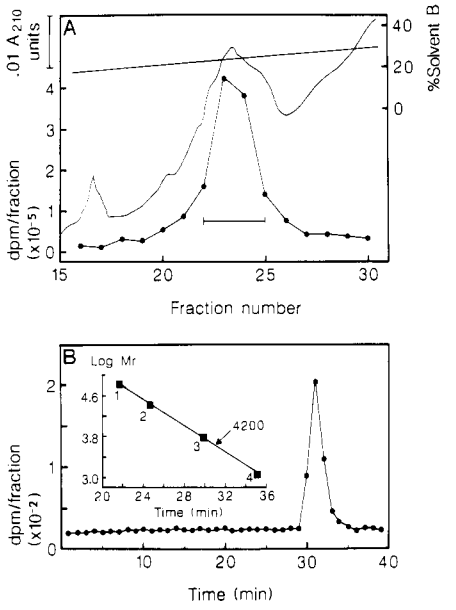

FIGURE 2: Repurification and apparent molecular weight determination of [^{3}H]DDF-labeled material in pool Ia. (A) Pool Ia (fractions 28–29) from Figure 1A was diluted with 2 volumes of 0.13% heptafluorobutyric acid and subjected to reversed-phase HPLC as described in Figure 1, except that 0.13% heptafluorobutyric acid replaced trifluoroacetic acid as counterion. Fractions (1.0 mL) containing the single peak of radioactivity (not shown) were pooled, diluted with 2 volumes of 0.1% trifluoroacetic acid, and rechromatographed exactly as described in Figure 1, yielding the absorbance (solid trace) and radioactivity (●) profiles shown here for the relevant portion of the chromatogram. The recoveries of injected radioactivity in the two reversed-phase HPLC analyses were 75 and 85%, respectively. The horizontal bar denotes fractions pooled (pool Ia1) for further analysis. (B) An aliquot (5 μL) of pool Ia1 [fractions 23–25 in (A)] was dried, redissolved in 100 μL of 8 M urea/10% acetic acid, and analyzed by gel permeation HPLC on one Model 250 and two Model 125 TSK columns connected in series (see Materials and Methods). Radioactivity was measured in 0.5-mL fractions of the column eluates (●). The recovery of injected radioactivity exceeded 90%. The elution times of markers for the void and total column volumes (keyhole limpet hemocyanin and dinitrophenol–lysine, respectively) were 19 and 43 min, as determined in separate analyses. The inset shows the linear relation obtained for Log molecular weight (M_r) vs elution time for standard proteins in the same system determined in parallel runs. The standards used were (1) bovine serum albumin (67 kDa), (2) chymotrypsinogen A (25 kDa), (3) insulin (5.7 kDa), and (4) gramicidin S (1.1 kDa). The arrow denotes the elution position and estimated molecular weight in this system of the [^{3}H]DDF-labeled component analyzed here.

(Table I). The amount of covalently bound radiolabel loaded onto the sequenator in this analysis, as calculated from the specific activity of the [^{3}H]DDF used for photolabeling, was 150 pmol, which is well above the detection limit for PTH amino acid; the identified sequence thus most probably corresponds to the [^{3}H]DDF-labeled peptide. On the basis of its apparent molecular weight of 4200 (Figure 2B), this peptide presumably extends to either Met-171 or Met-178, the next possible CNBr cleavage sites in the α-chain (calculated molecular weights 3100 and 3900, respectively).

An aliquot of material contained in pool Ib (Figure 1A), corresponding to approximately 130 pmol of covalently bound radiolabel, was subjected directly to sequence analysis. As shown in Table I, the same unique amino-terminal sequence identified in pool Ia1 was observed. gel permeation HPLC analysis (data not shown) indicated that the radiolabeled species in pool Ib also had an apparent molecular weight of approximately 4200. The radioactivity present in both pools Ia and Ib was thus associated with the fragment α 145–171 and/or 178.

Table I: Yields of PTH Amino Acids upon Sequence Analysis of Peak I Peptides[a]

	PTH amino acid (pmol)		
cycle	Ia1	Ib	Ib+
1	Lys (260)	Lys (2930)	Lys (3850)
2	Leu (260)	Leu (3160)	Leu (3000)
3	Gly (240)	Gly (2670)	Gly (2160)
4	Ile (230)	Ile (2390)	Ile (2240)
5		Trp (50)	Trp (810)
6	Thr (NQ)	Thr (830)	Thr (850)
7	Tyr (150)	Tyr (1220)	Tyr (1410)
8		Asp (830)	Asp (1000)
9	Gly (130)	Gly (820)	Gly (750)
10	Thr (NQ)	Thr (520)	Thr (660)
11	Lys (120)	Lys (650)	
12	Val (60)	Val (690)	
[^{3}H]DDF loaded (pmol)	150	130	20
initial yield (pmol)	330	3790	3880
repetitive yield (%)	89	83	81
starting position	α 145	α 145	α 145

[a] Material in pools Ia1 (Figure 2A), Ib, and Ib+ (parts A and B of Figure 1, respectively) were subjected to automated Edman degradation. For each analysis, PTH amino acids identified are designated by the conventional three-letter abbreviations and their yields in picomoles shown in parentheses. The amount of covalently bound [^{3}H]DDF loaded onto the sequenator was calculated from the specific activity of the [^{3}H]DDF employed for photolabeling. The initial and repetitive yields were calculated by linear regression analysis. The starting position denotes the position of the amino-terminal residue in the complete sequence of the α-chain. NQ denotes PTH amino acids identified but not quantifiable.

As shown in Table I, the specific radioactivity of the radiolabeled fragment was markedly different in the two pools. For pool Ia1, the initial yield of PTH amino acids was roughly 2-fold higher than the calculated amount of radiolabel loaded onto the sequenator (330 vs 150 pmol, respectively); comparable results were obtained for pool Ia before repurification (290 vs 170 pmol; data not shown). Pool Ib, on the other hand, showed an approximately 30-fold excess of PTH amino acids over the calculated amount of radiolabel loaded (3790 vs 130 pmol). It would thus appear that the radiolabeled fragment extending from αLys-145 was resolved into two components by reversed-phase HPLC, pool Ia comprising predominantly the [^{3}H]DDF-modified peptide separated from its unlabeled counterpart and pool Ib containing some radiolabeled material along with the vast majority of the unlabeled fragment.

The results of radioactivity measurements on the sequenator output for pools Ia1 and Ib are shown in Figure 3. In both cases, a clear release of tritium was observed at cycle 5, with tailing on cycle 6 that was compatible with the extent of carry-over of PTH amino acids associated with these analyses. Cycle 5 corresponds to αTrp-149 in the sequence of the identified α-subunit fragment extending from αLys-145; this residue was thus labeled by [^{3}H]DDF. In addition, a shoulder on cycle 7, which exceeds that expected solely from the sequence carry-over, was evident in the case of pool Ib. The corresponding residue αTyr-151 thus may represent a second site of labeling. No further release of radioactivity above background was observed in up to 30 cycles for either sample.

In order to verify at the sequence level that labeling of αTrp-149 (and possibly αTyr-151) was inhibited by agonist, material from the carbamoylcholine-protected batch corresponding to pool Ia before repurification (Ia+; fractions 30–31 in Figure 1B) and pool Ib (Ib+; fractions 33–35 in Figure 1B) was subjected separately to sequence analysis. Pool Ia$^+$ exhibited a single amino-terminal sequence corresponding to the non-AcChoR component present in pool Ia before repurification (data not shown); the sequence extending from αLys-

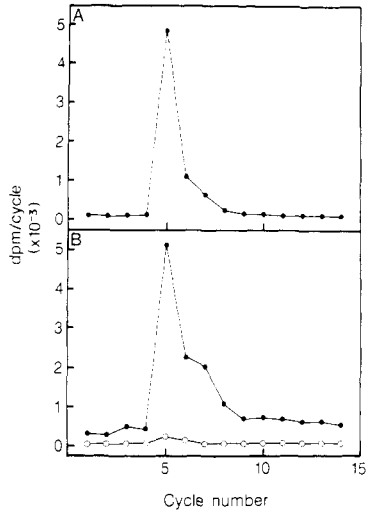

FIGURE 3: Radioactivity released on sequence analysis of CNBr fragments in pools Ia1 and Ib. (A) Repurified material contained in pool Ia1 (fractions 23–25 in Figure 2A) was subjected to automated sequence analysis; radioactivity associated with the PTH fraction at each cycle is shown (●). The sample loaded contained approximately 2.4×10^5 dpm, of which 4×10^4 dpm (17%) was recovered on the filter at the end of 30 cycles. The total radioactivity in the 30 cycles analyzed was 3×10^5 dpm (13% of the load); cycles 5–7 contained 30% of the recovered radioactivity. (B) Material contained in pool Ib (fractions 31–33 in Figure 1A) was sequenced and released radioactivity measured (●). Approximately 2.2×10^5 dpm was loaded, and 3.2×10^4 dpm (15%) remained on the filter after 25 cycles. The total radioactivity in the 25 cycles was 1.6×10^4 dpm (7% of the load); cycles 5–7 contained 25% of the recovered radioactivity. The radioactivity released upon sequencing of the corresponding material from the carbamoylcholine-protected sample (fractions 33–35 in Figure 1B) is also shown (○).

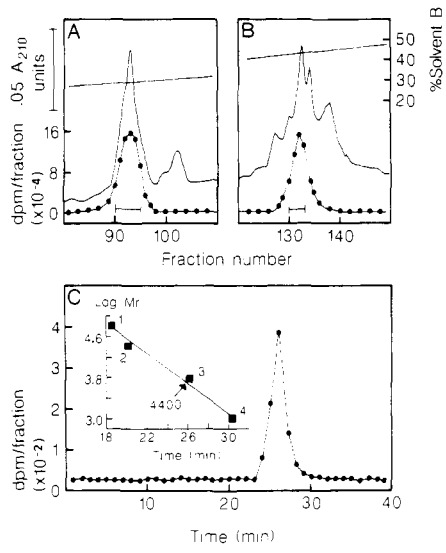

FIGURE 4: Repurification and apparent molecular weight determination of [^{3}H]DDF-labeled material in pools IIa and IIb. (A) Pool IIa (fractions 37–38) in Figure 1A was diluted with 2 volumes of 0.1% trifluoroacetic acid and rechromatographed in the same reversed-phase HPLC system. Fractions (1.0 mL) of the eluate were collected, and radioactivity was measured in 10-μL aliquots. The relevant portions of the UV_{210} absorbance (solid trace) and radioactivity (●) profiles are shown here; radioactivity is shown for each fraction from 89 to 98 and for every second fraction for the remainder of the profile. The horizontal bar denotes the fractions pooled (pool IIa1) for further characterization; pool IIa1 contained approximately 65% of the injected radioactivity. (B) Pool IIb (fractions 39–40) from Figure 1A was diluted with 2 volumes of 0.13% heptafluorobutyric acid and rechromatographed under identical conditions except that 0.13% heptafluorobutyric acid replaced 0.1% trifluoroacetic acid as counterion and a steeper elution gradient (0.5%/min) was employed. Remaining details were as described in (A). The radioactivity profile is shown for each fraction from 128 to 130 and for every second fraction for the remainder of the profile. The pool (IIb1) of fractions (131–133) denoted by the horizontal bar contained approximately 50% of the injected radioactivity. (C) An aliquot (10 μL) of pool IIa1 from (A) was dried, redissolved in 100 μL 8 M urea/10% acetic acid, and analyzed by gel permeation HPLC (details as for Figure 2B). The recovery of injected radioactivity exceeded 90%. The elution times of the void and total column markers, as measured in parallel runs, were 16 and 41 min, respectively.

145 was not present in detectable amounts in two separate analyses of pool Ia+. In light of results suggesting that pool Ia contained the [^{3}H]DDF-modified species resolved from its unlabeled counterpart, this finding provides indirect evidence that labeling of the identified α-subunit fragment was inhibited by carbamoylcholine. Direct support for this conclusion was obtained by sequence analysis of pool Ib+. In this case, the unique amino-terminal sequence extending from αLys-145 was observed in amounts comparable to those for the unprotected material (Table I), but the radioactivity associated with cycle 5, and also with cycle 7, was greatly reduced (Figure 3B). This result demonstrates unambiguously that photolabeling of αTrp-149 (and possibly also αTyr-151) by [^{3}H]DDF was inhibited by agonist.

Characterization of [^{3}H]DDF-Labeled Material in Peak II. The majority (approximately 60%) of the agonist-protectable labeling of the α-chain was associated with peak II (Figure 1A). We have previously reported that the predominant [^{3}H]DDF-labeled species present in this peak corresponds to the α-chain CNBr fragment α 179–207 (Dennis et al., 1986). In the present study, radiolabeled material in peak II was further characterized to identify the sites of incorporation of [^{3}H]DDF in this fragment.

It can be seen in Figure 1A that several UV_{210} absorbing components were associated with the rather broad peak of radioactivity comprising peak II. The central portion of the radioactive peak (fractions 37–40) was divided into two pools (IIa and IIb in Figure 1A) corresponding to two partially resolved UV_{210} absorbing species, and radiolabeled material in the two pools was analyzed separately.

Pool IIa (fractions 37–38 in Figure 1A), which coincided in the chromatogram with the summit of the peak of radioactivity, contained a minor UV_{210} absorbing component greatly reduced in the corresponding position of the chromatogram for the carbamoylcholine-protected sample (arrows in Figure 1A,B). Rechromatography of pool IIa in the same HPLC system yielded a peak of UV_{210} absorbing material containing all of the recovered radioactivity (Figure 4A). The fractions corresponding to the central portion of this peak (fractions 91–95 in Figure 4A) were pooled (pool IIa1), and an aliquot was analyzed by gel permeation HPLC. As shown in Figure 4C, pool IIa1 exhibited a single radiolabeled component of approximately 4400 apparent molecular weight.

Sequence analysis of material contained in pool IIa1 revealed two amino-terminal sequences: (1) a major sequence Lys-Asp-Tyr-Arg-Gly-Xaa... that corresponds to the α-subunit CNBr fragment extending from αLys-179 (cleavage at αMet-178); and (2) a minor sequence Glu-Ser-Gly-Glu-Xaa-Val... that corresponds to an overlapping CNBr fragment extending from αGlu-172 (cleavage at αMet-171), generated as a result of incomplete cleavage at αMet-178 (Table II).

Pool IIb (fractions 39–40 in Figure 1A) corresponded in the UV_{210} absorbance profile to a major species present in both the unprotected and carbamoylcholine-protected samples (cf. Figure 1B). Sequence analysis of an aliquot of pool IIb revealed the two amino-terminal sequences identified in pool IIa1 in roughly the same proportion (data not shown) but with initial yields that exceeded those for pool IIa1 by a factor of

Table II: Yields of PTH Amino Acids upon Sequence Analysis of Peak II Peptides[a]

cycle	PTH amino acid (pmol)					
	IIa1		IIb1		II+	
1	Lys (410)	Glu (100)	Lys (210)	Glu (40)	Lys (240)	Glu (108)
2	Asp (290)	Ser (20)	Asp (200)	Ser (10)	Asp (150)	
3	Tyr (170)	Gly (70)	Tyr (130)	Gly (40)	Tyr (190)	Gly (70)
4	Arg (110)	Glu (80)	Arg (30)	Glu (20)		Glu (50)
5	Gly (160)		Gly (110)	Xaa	Gly (160)	
6		Val (20)		Val (10)		Val (40)
7	Lys (100)		Lys (60)	Xaa	Lys (70)	
8	His (30)	Lys (60)	His (20)	Lys (30)	His (NQ)	Lys (30)
9		Asp (10)		Xaa		
10	Val (60)	Tyr (10)	Val (50)	Tyr (10)	Val (50)	
11	Tyr (60)		Tyr (50)		Tyr (40)	
12	Tyr (60)		Tyr (50)		Tyr (60)	
13	Thr (10)		Thr (10)		Thr (NQ)	
14						
15						
16	Pro (20)		Pro (10)		Pro (20)	
17	Asp (20)		Asp (20)			
18			Thr (10)			
19	Pro (30)		Pro (30)			
20	Tyr (30)		Tyr (20)			
21	Leu (30)					
22	Asp (30)					
23	Ile (20)					
24	Thr (10)					
25	Tyr (20)					
[^{3}H]DDF loaded (pmol)	160		90		20	
initial yield (pmol)	230	90	200	30	260	110
repetitive yield (%)	88	82	86	92	84	83
starting position	α 179	α 172	α 179	α 172	α 179	α 172

[a] Material contained in pools IIa1 (Figure 4A), IIb1 (Figure 4B), and II+ (Figure 1B) was subjected to automated Edman degradation. Details are as given in Table I.

10 when normalized to the original HPLC output. Furthermore, whereas the ratio of initial yield of PTH amino acids to the calculated amount of radiolabel loaded onto the sequenator was close to 2 for pool IIa1 (320 pmol/160 pmol; Table II), this value was greater than 10 for pool IIb (data not shown). This finding suggests that pool IIa was comprised predominantly of the [^{3}H]DDF-labeled species separated from the majority of the unlabeled counterparts that eluted in pool IIb, as observed for the radiolabeled fragment in peak I (see previous section).

Radiolabeled material in pool IIb was repurified by reversed-phase HPLC using heptafluorobutyric acid as counterion (details in legend to Figure 4). As shown in Figure 4B, several UV_{210} absorbing components were resolved in this system, one of which coeluted with the single peak of radioactivity. Gel permeation HPLC analysis of an aliquot of the repurified material (pool IIb1; fractions 131–133 in Figure 4B) yielded results identical with those obtained for pool IIa1, i.e., a single radiolabeled species of approximately 4400 apparent molecular weight (data not shown). Upon sequence analysis, pool IIb1 still showed the same two amino-terminal sequences identified in pool IIa1, a major sequence extending from αLys-179 and a minor one from αGlu-172 (Table II). The ratio of initial yield of PTH amino acids to the calculated amount of [^{3}H]DDF loaded in this case was approximately 2.5 as compared to 10 for pool IIb, indicating that the labeled and unmodified counterparts had been partially resolved upon repurification.

For both pools IIa1 and IIb1, the amount of radiolabel associated with the material subjected to sequence analysis (160 and 90 pmol, respectively; Table II) was sufficient to permit detection of PTH amino acids for the radiolabeled species. The covalently bound radioactivity present in pools IIa and IIb was thus most probably associated with the

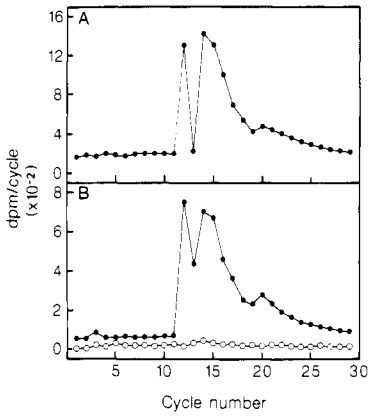

FIGURE 5: Radioactivity released on sequence analysis of CNBr fragments in pools IIa1 and IIb1. (A) Repurified material in pool IIa1 (fractions 91–95 in Figure 4A) was sequenced and released radioactivity measured (●). The sample loaded contained approximately 2.6×10^5 dpm; following 30 cycles, 4.7×10^4 dpm (18%) remained on the filter, with 1.2×10^4 dpm (5%) being recovered in the sequenator output. (B) Repurified material in pool IIb1 (fractions 131–133 in Figure 4B) was sequenced and released radioactivity measured (●). Approximately 1.4×10^5 dpm was loaded; following 30 cycles, 2.3×10^4 dpm (16%) remained on the filter, with 1.1×10^4 dpm (8%) being recovered in the sequenator output. Radioactivity released during sequence analysis of the entire pool II for the carbamoylcholine-protected sample (pool II+; fractions 38–42 in Figure 1B) is also shown (○).

overlapping α-chain CNBr fragments extending from αLys-179 and αGlu-172. On the basis of the apparent molecular weight of 4400 estimated by gel permeation HPLC, the radiolabeled species could not extend beyond the next possible CNBr cleavage site at αMet-207 (calculated molecular weight 3700 and 4500 for α 179–207 and α 171–207, respectively).

Measurements of the radioactivity released during sequence

analysis of pools IIa1 and IIb1 yielded the results shown in Figure 5. In both cases, no release over background was observed in cycles 1–11, while major peaks of tritium release were evident at cycles 12, 14, and 15, with marked tailing of the radioactivity in subsequent cycles and a slight rise at cycle 20. On the basis of the overlap for the two α-subunit sequences identified in pools IIa1 and IIb1, we can conclude that radioactivity released in cycles 12–18 represents labeling of the major CNBr fragment extending from αLys-179; the minor fragment from αGlu-172 could not have been the source of radioactivity in these cycles since no release of tritium over background was associated with the corresponding positions in the major fragment (i.e., cycles 5–11). The major peaks of radioactivity at cycles 12, 14, and 15 thus represent labeling by [^{3}H]DDF of αTyr-190, αCys-192, and αCys-193 within the fragment extending from αLys-179. The extent of tailing of radioactivity in cycles 16–18 observed for both samples and in cycle 13 for pool IIb1 was greater than that expected on the basis of carry-over of PTH amino acids associated with these cycles (15–20%), suggesting that the corresponding residues in the major fragment may have been labeled to some extent. The source of the radioactivity released at cycles 19 and onward in these analyses cannot be assigned with certainty. Tritium release in these cycles could conceivably reflect labeling of additional residues in the fragment extending from αLys-179 (particularly αTyr-198, corresponding to cycle 20) or the same region (i.e., αTyr-190 to αThr-196) in the overlapping fragment from αGlu-172.

In an effort to determine if all of the radioactivity present in peak II represented labeling of the same sites identified above, the ascending and descending extremities of the radioactive peak were subjected separately to sequence analysis (data not shown). The descending portion (fractions 41–42 in Figure 1A) exhibited the two α-subunit sequences extending from Lys-179 and Glu-172 and a profile of released radioactivity similar to that for IIa1 and IIb1. The ascending portion (fraction 36 in Figure 1A) yielded three amino-terminal sequences: a major sequence (Pro-Gln-Trp-Val-Arg...), corresponding to an α-chain CNBr fragment extending from Pro-309 (cleavage at Met-308), and two minor sequences that corresponded to the two distinct radiolabeled fragments already identified, i.e., that extending from αLys-179, as observed for the other peak II pools, and that from αLys-145, as identified in peak I. The profile of released radioactivity (not shown) resembled a superposition of those obtained for these two identified fragments with major peaks of tritium release at cycles 5, 12, 14, and 15. The most plausible interpretation of this result is that this pool of fractions contains the overlap region of peaks I and II (see Figure 1A). These findings thus indicate that all of the radiolabeled material eluting in peak II corresponds to labeling of the identified α-chain fragments.

That the labeled α-subunit residues identified in pools IIa and IIb incorporated [^{3}H]DDF in an agonist-sensitive manner is suggested by the marked decrease (by 85%) in radioactivity in the corresponding fractions obtained from the carbamoylcholine-protected sample (Figure 1). In order to test directly the labeling specificity, the fractions corresponding to pools IIa and IIb in the carbamoylcholine-protected sample (fractions 38–42 in Figure 1B) were pooled (pool II+), and an aliquot was subjected directly to sequence analysis. As shown in Table II, this material exhibited the two amino-terminal sequences extending from αLys-179 and αGlu-172, as observed for the unprotected sample, but showed no release of radioactivity above background (Figure 5B) throughout the analysis (30 cycles performed). This result demonstrates that

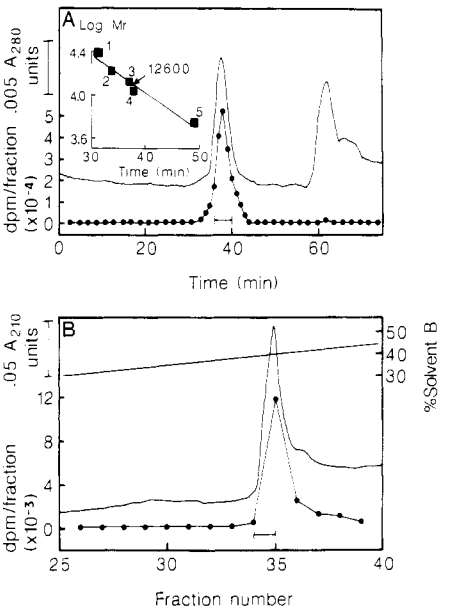

FIGURE 6: Repurification and apparent molecular weight determination of [^{3}H]DDF-labeled material in pool III. (A) Pool III (fractions 55–56) from Figure 1A was dried, redissolved in 200 μL of 8 M urea/10% acetic acid, and subjected to gel permeation HPLC on two Model 250 and one Model 125 TSK columns as described under Materials and Methods. Eluates were monitored for UV absorbance at 280 nm (solid trace) and radioactivity measured in 5-μL aliquots of fractions collected every minute. The radioactivity profile (●) is shown for each fraction from 33 to 44 min and every second fraction for the remainder of the profile. The horizontal bar indicates fractions (37–40) pooled for repurification. The void and total elution volumes measured as in Figure 2B were 29 and 64 min, respectively. The inset shows the calibration curve constructed by using the standard proteins (1) chymotrypsinogen A (25 kDa), (2) myoglobin (17.7 kDa), (3) ribonuclease A (14.3 kDa), (4) cytochrome c (12.5 kDa), and (5) insulin (5.7 kDa). The elution time and apparent molecular weight of the [^{3}H]DDF-labeled species are indicated by the arrow. The recovery of injected radioactivity exceeded 90%. (B) A portion (approximately $^1/_8$) of the pooled fractions (37–40) from (A) was diluted with 0.1% trifluoroacetic acid/18% 1-propanol and subjected to reversed-phase HPLC as described in Figure 1 except that (1) solvent B was 0.1% trifluoroacetic acid/90% 1-propanol, (2) equilibration and the start of the elution gradient were at 20% B, and (3) a steeper elution gradient (0.5%/min) was employed. Radioactivity was measured in aliquots (10 μL) of fractions taken every min (●) and UV_{210} absorbance monitored (solid trace); the relevant portions of the corresponding profiles are shown. The recovery of injected radioactivity was approximately 65% in this analysis. The horizontal bar indicates the material (pool III1; fraction 35) taken for amino acid sequence and composition analyses.

the incorporation of [^{3}H]DDF into all of the α-subunit residues shown to be labeled in the fragment α 179–207 was inhibited by carbamoylcholine.

Characterization of [^{3}H]DDF-Labeled Material in Peak III. Approximately 5% of the carbamoylcholine-protectable labeling of the α-chain was recovered in peak III following reversed-phase HPLC of the CNBr digests (Figure 1). Two partially resolved UV_{210} absorbing components eluted in fractions corresponding to peak III, the majority of the radioactivity being associated with the earlier eluting species.

Sequence analysis of this material (fractions 55–56 in Figure 1A) revealed two amino-terminal sequences (data not shown), a major one (Ser-Glu-His-Glu-Thr...) corresponding to the amino terminus of the mature α-subunit (Devillers-Thiéry et al., 1979) and a minor sequence (Thr-Lys-Leu-Leu-Leu...) corresponding to a CNBr fragment extending from αThr-106 (cleavage at Met-105). On the basis of the calculated amount of radiolabel loaded onto the sequenator (75 pmol), it is highly probable that the radiolabeled fragment corresponded to one

Table III: Yields of PTH Amino Acids upon Sequence Analysis of Pool III1[a]

cycle	PTH amino acid (pmol)	cycle	PTH amino acid (pmol)
1	Ser (90)	6	Arg (NQ)
2	Glu (70)	7	Leu (40)
3	His (10)	8	Val (20)
4	Glu (60)	9	Ala (50)
5	Thr (20)	10	Asn (40)

[a] Material in pool III1 from Figure 6B, containing approximately 3 × 10^4 dpm (20 pmol of radiolabel), was subjected to automated Edman degradation. The apparent repetitive and initial yields for the sequence, as calculated by linear regression analysis, were 97% and 80 pmol, respectively. Following 30 cycles, 1.5 × 10^4 dpm (50% of load) was recovered on the filter. Other details are as in Table I.

of the two identified sequences.

Material contained in pool III was repurified by using the gel permeation HPLC system (details in the legend to Figure 6). A peak of UV_{280} absorbing material containing essentially all of the injected radioactivity eluted at 38 min in this system (Figure 6A), corresponding to an apparent molecular weight of approximately 12 600 (inset to Figure 6A). When this component (fractions 37–40) was rechromatographed by reversed-phase HPLC (see legend to Figure 6), a single peak of UV_{210} absorbing material was observed that coeluted with the peak of radioactivity (Figure 6B).

Sequence analysis of the repurified material (pool III1; fraction 35 in Figure 6B) revealed the single amino-terminal sequence extending from αSer-1 (Table III), with no detectable amounts of the sequence from αThr-106. The amount of radiolabel loaded onto the sequenator (20 pmol) should have been sufficient to permit detection of the [^{3}H]DDF-modified species by analysis of PTH amino acids. The fact that the radioactivity eluted with the sequenced material in both reversed-phase and gel permeation HPLC systems further supports the conclusion that the [^{3}H]DDF-labeled peptide corresponds to the identified sequence extending from αSer-1.

Judging from its apparent molecular weight of approximately 12 600 (Figure 6A), the radiolabeled species could extend to either of the next two possible CNBr cleavage sites at Met-105 or Met-117 (calculated molecular weights 12 600 and 14 000, respectively), but clearly does not include the segment extending to Met-144 [calculated molecular weight = 17 500 plus approximately 2000 for the oligosaccharide attached to Asn-141; see Merlie and Smith (1986)]. As a further test for the identity of the carboxy terminus, the repurified material was subjected to amino acid analysis. Comparison of the observed amino acid composition with that expected for fragments extending from αSer-1 to potential CNBr cleavage sites at Met-105, -117, and -144 provided a best fit for the fragment α 1–105 (Table IV). The absence of detectable Met in this analysis supports the view that the sequenced material contained no uncleaved Met residues. We thus conclude that the CNBr fragment α 1–105 contains an additional site of [^{3}H]DDF incorporation distinct from those identified in peaks I and II.

When radioactivity was measured in the sequenator output following analysis of the total pool III and the repurified pool III1, no release of tritium above background was observed for either sample in up to 30 cycles (data not shown). The [^{3}H]DDF-labeled amino acids are thus presumably located between αIle-31 and αMet-105. Although it was not possible to demonstrate the agonist sensitivity of labeling at the amino acid level, the fact that radioactivity associated with peak III was reduced by approximately 75% in the carbamoylcholine-protected batch (cf. parts A and B of Figure 1) clearly indicates that the incorporation of [^{3}H]DDF into this segment was inhibited by agonist.

Table IV: Comparison of Experimentally Determined Amino Acid Composition of Material in Pool III1 with That Predicted for α-Subunit Fragments

	x	α 1–105	α 1–117	α 1–144	α 1–171
Cys	0	0 (0)	0 (0)	0 (2)	0 (2)
Asx	1.393	16.71 (18)	20.90 (19)	20.90 (21)	23.68 (24)
Thr	0.369	4.43 (4)	5.54 (6)	5.54 (9)	6.27 (12)
Ser	0.221	2.65 (2)	3.32 (2)	3.32 (3)	3.76 (7)
Glx	0.926	11.11 (11)	13.89 (11)	13.89 (14)	15.74 (15)
Pro	0.328	3.94 (4)	4.92 (4)	4.92 (7)	5.58 (9)
Gly	0.426	5.11 (4)	6.39 (5)	6.39 (5)	7.24 (7)
Ala	0.352	4.22 (4)	5.28 (4)	5.28 (5)	5.98 (5)
Val	1.0	12 (13)	15 (13)	15 (14)	17 (15)
Met	0	0 (0)	0 (1)	0 (2)	0 (3)
Ile	0.590	7.08 (9)	8.85 (10)	8.85 (13)	10.03 (15)
Leu	1.0	12 (12)	15 (15)	15 (15)	17 (17)
Tyr	0.213	2.56 (3)	3.20 (4)	3.20 (5)	3.62 (6)
Phe	0.148	1.78 (2)	2.22 (2)	2.22 (5)	2.52 (6)
His	0.361	4.33 (5)	5.41 (5)	5.41 (6)	6.14 (6)
Lys	0.295	3.54 (3)	4.43 (5)	4.43 (6)	5.02 (8)
Arg	0.549	6.59 (7)	8.24 (7)	8.24 (7)	9.33 (8)
Δ[c]		1.78	3.86	4.97	5.62

[a] Material contained in pool III1 (Figure 6B) was subjected to amino acid composition analysis. The amounts of each amino acid are normalized to Leu = 1 mol/mol; values shown here are from a single analysis. [b] For each fragment of the α-chain considered here, the values in parentheses denote the number of residues present in the peptide as predicted from the known sequence of α-chain from *T. marmorata*. For comparison, the results of the experimental amino acid composition analysis are shown normalized to the number of Leu residues predicted for the peptide. [c] This index is the sum, for all the amino acids, of the percentage of difference between predicted and experimental values. A better fit corresponds to a lower value of Δ and a perfect fit to Δ = 0.

Discussion

The AcChoR possesses two "primary" AcCho-binding sites that bind nicotinic agonists, competitive antagonists, and snake venom α-toxins in a mutually exclusive manner (Weber & Changeux, 1974; Neubig & Cohen, 1979, 1980). Evidence presented in the accompanying paper (Langenbuch-Cachat et al., 1988) shows that, under appropriate conditions, this pair of sites can be selectively labeled on the native AcChoR with the photoactivable aryldiazonium derivative [^{3}H]DDF.

In the present study, radioactivity associated with the α-chain isolated from AcChoR-rich membranes following preparative photolabeling with [^{3}H]DDF was decreased by roughly 70% in the presence of 100 μM carbamoylcholine. The labeling stoichiometry approximated one molecule of reagent incorporated in an agonist-protectable manner per inactivated α-BgTx-binding site. As previously reported (Dennis et al., 1986), reversed-phase HPLC analysis of CNBr digests of the [^{3}H]DDF-labeled α-chain yielded three peaks (I–III) of radioactivity that markedly decreased (by 75–85%) when photolabeling was performed in the presence of carbamoylcholine. Amino acid composition and/or amino-terminal sequence analyses of repurified peptides, as well as apparent molecular weight determinations by gel permeation HPLC, revealed that these three radioactive peaks represented labeling of distinct, nonoverlapping CNBr fragments of the α-chain (see Figure 7A).

Radiolabeled material in peak II, which accounted for approximately 60% of the agonist-protectable labeling of the α-chain, was shown to be comprised predominantly of the fragment α 179–207. The results of sequence analyses show unambiguously that Tyr-190, Cys-192, and Cys-193 were labeled by [^{3}H]DDF and indicate that additional residues located between Tyr-190 and Met-207, particularly Tyr-198,

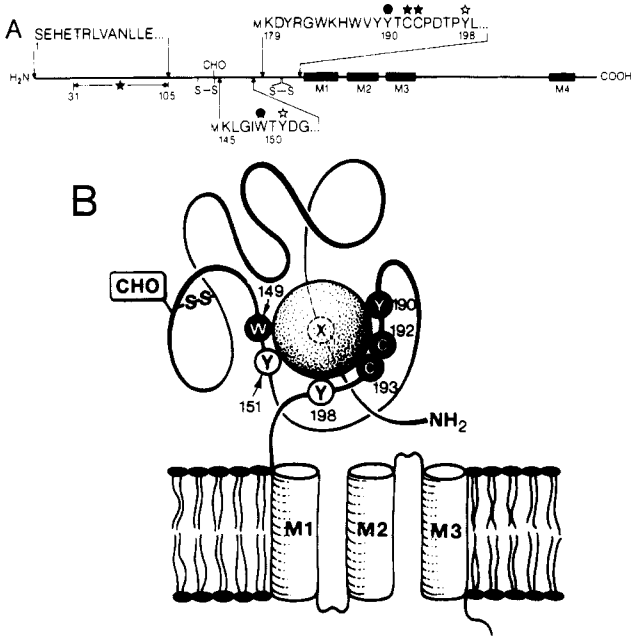

FIGURE 7: (A) Locations of [^{3}H]DDF-labeled residues within the α-chain primary structure. In this schematic representation of the α-chain, black boxes indicate the four hydrophobic segments (M1–M4), CHO indicates the oligosaccharide side-chain linked to Asn-141, and S–S indicates the disulfide bonds believed to link Cys-128–142 and Cys-192–193, respectively. The identified [^{3}H]DDF-labeled CNBr fragments are localized along the sequence of the α-chain; residues shown unambiguously to incorporate [^{3}H]DDF in an agonist-protectable manner are indicated by filled stars, while open stars denote residues for which suggestive evidence for labeling was obtained. The exact residue(s) labeled in the segment α 31–105 is (are) unknown. (B) Schematic model for the proposed folding of the amino-terminal extracellular segment of the α-chain in the AcChoR oligomer. This cartoon shows a portion of the α-chain, including the hydrophilic segment α 1–210, which is assigned to the synaptic cleft, and the three hydrophobic segments M1–M3, depicted as membrane-spanning α-helices. The large sphere represents the space occupied by a molecule of DDF in all possible orientations within its binding site (see text). The polypeptide chain has been folded in such a way that the [^{3}H]DDF-labeled residues, indicated by the standard one-letter codes, are in contact with the sphere. Filled circles denote those residues unambiguously shown to be labeled and open circles those for which suggestive evidence for labeling was obtained. Numbers refer to the positions of the labeled residues within the sequence of the α-chain. The X denotes the unidentified [^{3}H]DDF-labeled residue(s) located within the segment α 31–105. The disulfide bond linking αCys-128 and αCys-142 (S–S) and the site of N-linked glycosylation at Asn-141 (CHO) are indicated. No specific assumptions concerning the secondary or tertiary structures, other than the proximity of the [^{3}H]-DDF-labeled residues, are implied. The disulfide bonding arrangement is taken from Kao and Karlin (1986).

may also have incorporated the reagent to some extent.

The [^{3}H]DDF-labeled peptide corresponding to peak I, which represented approximately 5% of the agonist-protectable labeling of the α-chain, was identified as the CNBr fragment α 145–171 (though we cannot exclude heterogeneity at the carboxy terminus). Sequence analysis demonstrated that Trp-149 and possibly also Tyr-151 were labeled by [^{3}H]DDF in this segment of the α-chain.

The results obtained for peaks I and II indicated that the [^{3}H]DDF-modified species were partially resolved from their unmodified counterparts by reversed-phase HPLC. In both cases, the labeled peptides appeared to elute slightly earlier than the corresponding unlabeled fragments, possibly as a result of the additional positive charge contributed by the covalently bound phenyldimethylamino group, which would be protonated at the pH used for reversed-phase separations (pH 2.1). The separation of the [^{3}H]DDF-modified and -unmodified peptides of the same sequence was not a serious obstacle, since the radiolabeled species in peaks I and II were recovered in sufficient amounts for sequence analyses. Sequencing of the corresponding unlabeled fragments from the carbamoylcholine-protected sample showed unambiguously that all of the [^{3}H]DDF-modified amino acids identified in peaks I and II were labeled in an agonist-protectable manner.

The recovery of radioactivity in the sequenator output following sequence analysis of labeled peptides in peaks I and II was in all cases quite low (5–12% of load). This was presumably not due to amino-terminal blockage of the labeled fragments since the radioactivity remaining on the filter was not excessive. Problems in the recovery of covalently labeled PTH amino acids from the gas-phase sequenator have been noted in other cases (Russo et al., 1985; Giraudat et al., 1986) and may reflect technical difficulties particular to the modified residues.

The covalently bound radioactivity present in peak III, which accounted for approximately 5% of the agonist-protectable labeling of the α-chain, was shown to be associated with a large fragment extending from αSer-1, probably to the next possible CNBr cleavage site at αMet-105. Owing to the size of the radiolabeled species and despite several attempts at subcleavage, it was not possible to identify the specific amino acids modified by [^{3}H]DDF in this fragment; however, the results indicate that the covalently bound label lies beyond the Asp residue at cycle 30. The fact that radioactivity associated with peak III was decreased (by approximately 75%) in the carbamoylcholine-protected sample indicates that labeling of some residue(s) in the segment α 31–105 was inhibited by agonist.

The remainder (approximately 30%) of the agonist-protectable labeling of the α-chain by [^{3}H]DDF was associated with highly hydrophobic material that also contained the majority of the nonspecific labeling. Although we cannot exclude that this fraction could contain some agonist-sensitive labeling at sites distinct from those described above, it is highly probable that this material contains partial CNBr cleavage products in which one or more of the identified sites of [^{3}H]DDF incorporation are present in fragments containing hydrophobic regions at the carboxy terminus (for example, partial cleavage of the Met–Gln bond at position α 207–208 would generate the heavily labeled fragment α 179–207 attached to the hydrophobic segment M1).

The results of sequence analyses indicate that differences in the amounts of radioactivity associated with the labeled fragments corresponding to the major (peak II) and minor (peaks I and III) radioactive peaks can be attributed in large part to the number of labeled residues in each fragment rather than to the extent of [^{3}H]DDF incorporation at a given amino acid. While it is difficult to estimate the yield of labeling of each residue on the native AcChoR directly from the sequence data, the finding that the fragment α 179–207 contained three unambiguously labeled amino acids while the fragment α 145–171 contained only one indicates that the labeling yield per residue was within a factor of 5 in each of these fragments.

Two lines of evidence suggest that the identified [^{3}H]-DDF-modified residues are related to the pair of primary AcCho-binding sites. First, labeling of amino acids in the segments α 31–105, α 149–151, and α 190–198 was inhibited by 100 μM carbamoylcholine, and results obtained by Cohen and Strnad (1987) show that the primary sites are the only detectable agonist-binding sites at AcCho concentrations up to 1 mM. Second, covalent labeling of the native AcChoR by [^{3}H]DDF is almost exclusively a light-dependent reaction (Langenbuch-Cachat et al., 1988). Given the extremely high reactivity and short half-life ($<10^{-8}$ s) of the photogenerated

aryl cation intermediate (Ambroz & Kemp, 1979, 1982; Himashima et al., 1985; Grieve et al., 1985; Kieffer et al., 1986), [^{3}H]DDF would be expected, upon photolysis, to label any amino acid functional groups in the immediate vicinity of the bound reagent without significant diffusion of the reactive species, the aqueous solvent serving as "scavenger". This view is supported by recent studies with DDF complexed reversibly to crown ethers, which indicate that the reactive intermediate does not have time to leave the complex before alkylation occurs (M. Goeldner, C. Hirth, and J. P. Behr, personal communication). Taken together, these findings support the view that the α-chain residues shown to be labeled by [^{3}H]DDF in an agonist-protectable manner lie within or immediately adjacent to the primary AcCho-binding sites on the native AcChoR.

Since the regions of the AcChoR that form the AcCho-binding sites must be exposed to the synaptic cleft, it follows that the α-subunit residues labeled by [^{3}H]DDF in an agonist-protectable manner are localized on the extracellular portion of the polypeptide in the functional oligomer. Such a disposition is consistent with the transmembrane topology proposed on the basis of hydropathy analyses of the α-chain sequence (Noda et al., 1982; Devillers-Thiéry et al., 1983) but seems incompatible with the recent proposal, derived from immunochemical studies, that the segment α 143–151 forms an extended membrane-spanning structure, thus placing the [^{3}H]DDF-labeled residue αTrp-149 within the bilayer near the cytoplasmic face (Criado et al., 1985). The source of this discrepancy, which presumably reflects differences in experimental approaches, remains to be determined.

Previous studies based on affinity labeling of the reduced AcChoR with sulfhydryl-directed reagents (Kao et al., 1984) and α-toxin binding to denatured fragments or synthetic peptides of the α-subunit (Wilson et al., 1984, 1985; Neumann et al., 1985; 1986a,b; Mulac-Jericevic & Atassi, 1986; Ralston et al., 1987), as well as deletion mutants of the α-chain (Barkas et al., 1987), provided evidence that the region surrounding αCys-192 and -193 is located in or near the binding site for cholinergic ligands. The fact that the same region (i.e., α 190–198) represents the major target of agonist-protectable [^{3}H]DDF incorporation on the native AcChoR, as shown in the present study, points to an important contribution of this portion of the α-chain to the AcCho-binding sites on the native oligomer. The identification of the segments α 31–105 and α 149–151 as additional targets of agonist-protectable labeling by [^{3}H]DDF raises the possibility that these portions of the α-subunit may also contribute to the binding sites for cholinergic ligands on the native receptor. Such a possibility is consistent with evidence, derived from analyses of α-toxin and agonist/competitive antagonist binding to "renatured" (Tzartos & Changeux, 1984) and newly synthesized α-subunit [reviewed by Merlie and Smith (1986)], indicating that the high-affinity binding of α-toxin and its sensitivity to cholinergic ligands required an appropriate tertiary folding of the polypeptide chain.

The evidence supports the view that the agonist-protectable incorporation of [^{3}H]DDF into the three distinct α-chain segments occurs via the pair of primary AcCho binding sites. However, although the two α-subunits per AcChoR are encoded by a single gene (Merlie et al., 1983; Klarsfeld et al., 1984) and are thus most probably identical in primary structure, it is known that the two AcCho binding sites are pharmacologically nonequivalent [reviewed in Karlin (1983) and Culver et al. (1984)]. In addition, both sites undergo an allosteric transition from a state of low-affinity binding to a high-affinity state at equilibrium in the presence of agonists and of other ligands, in particular the noncompetitive blockers that stabilize the high-affinity state to varying extents [reviewed by Changeux et al. (1984)]. Under the conditions employed for photolabeling in the present study, i.e., in the presence of 100 μM phencyclidine, the low- and high-affinity states would be expected to be present in roughly equal proportions (Heidmann et al., 1983). The results obtained in the accompanying study (Langenbuch-Cachat et al., 1988) indicate that the two AcCho-binding sites, in both low- and high-affinity conformers, can be labeled by [^{3}H]DDF, with a mean stoichiometry of one molecule of reagent incorporated in an agonist-protectable manner per inactivated α-toxin-binding site. While we cannot exclude that the pharmacological heterogeneity exhibited by these sites could be reflected in the pattern of labeling and despite the fact that labeling of a given amino acid falls within the experimental error for the measured 1:1 stoichiometry, the simplest interpretation of the present findings is that all of the identified [^{3}H]DDF-labeled residues lie adjacent to a single molecule of [^{3}H]DDF bound to one AcCho-binding site. Assuming that the bound reagent could take up any number of possible orientations within this site, the rigid DDF molecule would occupy a sphere whose diameter equals the largest dimension of the ligand (approximately 12 Å). On the basis of this single-site interpretation, the various α-subunit residues that incorporate [^{3}H]DDF in an agonist-protectable manner would lie on the surface of this sphere and thus be brought within approximately 12 Å of one another by tertiary folding of the polypeptide chain in the native AcChoR (see model in Figure 7B).

The present findings raise the possibility that at least certain of the α-chain amino acids shown to incorporate [^{3}H]DDF in an agonist-protectable manner may be directly involved in agonist binding to the AcChoR. It is significant in this regard that four of the [^{3}H]DDF-labeled residues, namely, αTrp-149, αTyr-190, Cys-192, and Cys-193, are conserved in the α-subunits of muscle AcChoR from all species examined to date [reviewed by Stroud and Finer-Moore (1985)] and in the putative ganglionic α-subunit identified in the cell line PC 12 (Boulter et al., 1986) and are also present at homologous positions (Trp-153, Tyr-194, Cys 196, and Cys-197) in the putative neuronal α-chains from rat brain (Goldman et al., 1987). These residues are absent, however, from the corresponding portions of the other AcChoR subunits (Noda et al., 1983), consistent with a functional role particular to the α-chain.

Structure–activity studies (Michelson & Ziemal, 1973) have shown that the positively charged ammonium group of agonists/competitive antagonists is essential for binding activity via interactions with an electronegative subsite within the AcCho-binding site. Although resonance theory predicts that the positive charge carried by DDF would be shared by different parts of the molecule, the available evidence suggests that the cationic moiety imparting affinity for this subsite is provided by the diazonium function itself (Mautner & Bartels, 1970). On this basis, [^{3}H]DDF might be expected to label amino acids directly involved in complexing the quaternary ammonium group.

It has been widely held [reviewed by Luyten (1986)] that carboxylate anions on the AcChoR would be responsible for binding the cationic head group of AcCho, a view indirectly supported by crystallographic analyses of phosphocholine-specific antibodies (Padlan et al., 1976). The fact that Glu or Asp residues were not among the major [^{3}H]DDF-labeled residues identified in this work (although minor labeling of

αAsp-195 and/or αAsp-200 cannot be ruled out completely) may thus be significant. This did not appear to result from a selective loss of ester derivatives, since the corresponding methyl ester (*p*-acetoxydimethylaniline) was found to be stable under conditions used for CNBr cleavage and Edman degradation (data not shown). If acidic residues do incorporate [^{3}H]DDF in an agonist-protectable manner, then these residues are presumably located within the unsequenced radiolabeled segment α 31–105 or on the other AcChoR subunits. We cannot rule out the possibility, however, that residues located in proximity to the bound [^{3}H]DDF may not have been labeled to a detectable extent due to the existence of favored orientations of DDF within its binding site.

One interpretation consistent with the present findings is that the electronegative character of the quaternary ammonium binding domain is contributed, at least in part, by the lone pair electrons of the phenolic oxygen of αTyr-190, of the sulfur atoms forming the αCys-192–193 disulfide, and of the nitrogen atom of αTrp-149. Consistent with this possibility, crystallographic studies have shown that uncharged, dipolar functional groups, such as hydroxyls, can coordinate to the sphere of positive charge of the quaternary ammonium (Rosenfield & Murray-Rust, 1982).

In view of the fact that DDF acts as a competitive antagonist (Langenbuch-Cachat et al., 1988), the present findings provide no information on the mechanism by which AcCho triggers the ion-channel response; they do, however, permit the identification of specific amino acids that may be involved in the reversible binding of AcCho to its sites. A detailed picture of the interactions involved in agonist binding and the events underlying channel gating will be obtained only by a combination of experimental approaches and, ultimately, by solution of the crystal structure of agonist–AcChoR complexes.

ACKNOWLEDGMENTS

We thank Drs. Vanhove and Rousseau for tritiating the DDF precursor, Dr. A. Jaganathen for phencyclidine, R. Knecht, O. Seegmüller, and N. Franco for performing sequence analyses, and C. Henderson, A. Klarsfeld, and F. Revah for critical reading of the manuscript. Certain of the chemical analyses were carried out in the laboratory of Dr. D. Strosberg, Institut Pasteur, Paris.

Registry No. Trp, 73-22-3; Cys, 52-90-4; acetylcholine, 51-84-3.

REFERENCES

Ambroz, H. B., & Kemp, J. J. (1979) *Chem. Soc. Rev. 8*, 353–365.

Ambroz, H. B., & Kemp, J. J. (1982) *Chem. Commun.*, 172–173.

Barkas, T., Mauron, A., Roth, B., Alliod, C., Tzartos, S., & Ballivet, M. (1987) *Science (Washington, D.C.) 235*, 77–80.

Boulter, J., Evans, K., Goldman, D., Martin, G., Treco, D., Heinemann, S., & Patrick, J. (1986) *Nature (London) 319*, 368–374.

Changeux, J. P., Devillers-Thiéry, A., & Chemouilli, P. (1984) *Science (Washington, D.C.) 225*, 1335–1345.

Cohen, J. B., & Strnad, N. P. (1987) in *Molecular Mechanisms of Desensitization to Signal Molecules* (Konijn, T. M., Ed.) pp 257–273, Springer-Verlag, Berlin.

Criado, M., Hochschwender, S., Sarin, V., Fox, J. L., & Lindstrom, J. (1985) *Proc. Natl. Acad. Sci. U.S.A. 82*, 2004–2008.

Culver, P., Fenical, W., & Taylor, P. (1984) *J. Biol. Chem. 259*, 3763–3770.

Dabre, A. (1986) in *Practical Protein Chemistry—A Handbook* (Dabre, A., Ed.) pp 227–335, Wiley, Chichester, U.K.

Dennis, M., Giraudat, J., Kotzyba-Hibert, F., Goeldner, M., Hirth, C., Chang, J. Y., & Changeux, J. P. (1986) *FEBS Lett. 207*, 243–249.

Devillers-Thiéry, A., Changeux, J. P., Paroutaud, P., & Strosberg, A. D. (1979) *FEBS Lett. 104*, 99–105.

Devillers-Thiéry, A., Giraudat, J., Bentaboulet, M., & Changeux, J. P. (1983) *Proc. Natl. Acad. Sci. U.S.A. 80*, 2067–2071.

Gershoni, J. M., Hawrot, E., & Lentz, T. L. (1983) *Proc. Natl. Acad. Sci. U.S.A. 80*, 4973–4977.

Giraudat, J., Dennis, M., Heidmann, T., Chang, J. Y., & Changeux, J. P. (1986) *Proc. Natl. Acad. Sci. U.S.A. 83*, 2719–2723.

Goldman, D., Deneris, E., Luyten, W., Kochhar, A., Patrick, J., & Heinemann, S. (1987) *Cell (Cambridge, Mass.) 48*, 965–973.

Grieve, D. M., Graham, L. E., Ravenscroft, L. E., Skrabal, M. D., Sonoda, T., Szele, I., & Zollinger, H. (1985) *Helv. Chim. Acta 68*, 1427–1443.

Haggerty, J. G., & Froehner, S. C. (1981) *J. Biol. Chem. 256*, 8294–8297.

Heidmann, T., Oswald, R. E., & Changeux, J.-P. (1983) *Biochemistry 22*, 3112–3127.

Himashima, Y., Kobayashi, H., & Sonoda, T. (1985) *J. Am. Chem. Soc. 107*, 5286–5288.

Hucho, F. (1986) *Eur. J. Biochem. 158*, 211–226.

Kao, P. N., & Karlin, A. (1986) *J. Biol. Chem. 261*, 8085–8088.

Kao, P., Dwork, A., Kaldany, R., Silver, M., Wideman, J., Stein, S., & Karlin A. (1984) *J. Biol. Chem. 259*, 11662–11665.

Karlin, A. (1969) *J. Gen. Physiol. 54*, 245–264.

Karlin, A. (1983) *Neurosci. Comment. 1*, 111–123.

Kieffer, B., Goeldner, M., Hirth, C., Aebersold, R., & Chang, J. Y. (1986) *FEBS Lett. 202*, 91–96.

Klarsfeld, A., Devillers-Thiéry, A., Giraudat, J., & Changeux, J. P. (1984) *EMBO J. 3*, 35–41.

Knecht, R., Seegmüller, U., Liersch, M., Fritz, H., Braun, D. G., & Chang, J. Y. (1983) *Anal. Biochem. 130*, 65–71.

Laemmli, U. K. (1970) *Nature (London) 227*, 680–685.

Langenbuch-Cachat, J., Bon, C., Mulle, C., Goeldner, M., Hirth, C., & Changeux, J.-P. (1988) *Biochemistry* (preceding paper in this issue).

Lazure, C., Seidah, N. G., Chrétien, M., Lallier, R., & St-Pierre, S. (1983) *Can. J. Biochem. Cell Biol. 61*, 287–292.

Luyten, W. (1986) *J. Neurosci. Res. 16*, 51–73.

Mautner, H. G., & Bartels, E. (1970) *Proc. Natl. Acad. Sci. U.S.A. 67*, 74–78.

McCarthy, M. P., Earnest, J. P., Young, E. F., Choe, S., & Stroud, R. M. (1986) *Annu. Rev. Neurosci. 9*, 383–413.

Merlie, J. P., & Smith, M. M. (1986) *J. Membr. Biol. 91*, 1–10.

Merlie, J. P., Sebbane, R., Gardner, S., & Lindstrom, J. (1983) *Proc. Natl. Acad. Sci. U.S.A. 80*, 3845–3849.

Michelson, M., & Zeimal, E. (1973) in *Acetylcholine, an Approach to the Molecular Mechanism of Action*, pp 73–123, Pergamon, Oxford, U.K.

Mishina, M., Kurosaki, T., Tobimatsu, T., Morimoto, Y., Noda, M., Yamamoto, T., Terao, M., Lindstrom, J., Takahashi, T., Kuno, M., & Numa, S. (1984) *Nature (London) 307*, 604–608.

Mulac-Jericevic, B., & Atassi, M. Z. (1986) *FEBS Lett. 199*, 68–74.

Neubig, R. R., & Cohen, J. B. (1979) *Biochemistry 18*, 5464–5475.
Neubig, R. R., & Cohen, J. B. (1980) *Biochemistry 19*, 2770–2779.
Neubig, R. R., Krodel, E. K., Boyd, N. D., & Cohen, J. B. (1979) *Proc. Natl. Acad. Sci. U.S.A. 76*, 690–694.
Neumann, D., Gershoni, J. M., Fridkin, M., & Fuchs, S. (1985) *Proc. Natl. Acad. Sci. U.S.A. 82*, 3490–3493.
Neumann, D., Barchan, D., Safran, A., Gershoni, J. M., & Fuchs, S. (1986a) *Proc. Natl. Acad. Sci. U.S.A. 83*, 3008–3011.
Neumann, D., Barchan, D., Fridkin, M., & Fuchs, S. (1986b) *Proc. Natl. Acad. Sci. U.S.A. 83*, 9250–9253.
Noda, M., Takahashi, H., Tanabe, T., Toyosato, M., Furutani, Y., Hirose, T., Asai, M., Inayama, S., Miyata, T., & Numa, S. (1982) *Nature (London) 299*, 793–797.
Noda, M., Takahashi, H., Tanabe, T., Toyosato, M., Kikyotani, S., Furutani, Y., Hirose, T., Takashima, H., Inayama, S., Miyata, T., & Numa, S. (1983) *Nature (London) 302*, 528–532.
Padlan, E. A., Davies, D. R., Rudikoff, S., & Potter, M. (1976) *Immunochemistry 13*, 945–949.
Pedersen, S. E., Dreyer, E. B., & Cohen, J. B. (1986) *J. Biol. Chem. 261*, 13735–13743.
Popot, J. L., & Changeux, J. P. (1984) *Physiol. Rev. 64*, 1162–1184.
Ralston, S., Sarin, V., Thanh, H. L., Rivier, J., Fox, J. L., & Lindstrom, J. (1987) *Biochemistry 26*, 3261–3266.
Rosenfield, R. E., Jr., & Murray-Rust, P. (1982) *J. Am. Chem. Soc. 104*, 5427–5430.
Russo, M. W., Lukas, T. J., Cohen, S., & Stroud, J. V. (1985) *J. Biol. Chem. 260*, 5205–5208.
Saitoh, T., Oswald, R., Wennogle, L. P., & Changeux, J. P. (1980) *FEBS Lett. 116*, 30–36.
Stroud, R. M., & Finer-Moore, J. (1985) *Annu. Rev. Cell Biol. 1*, 317–351.
Tzartos, S. J., & Changeux, J. P. (1983) *EMBO J. 2*, 381–387.
Tzartos, S. J., & Changeux, J. P. (1984) *J. Biol. Chem. 259*, 11512–11519.
Walker, J. W., Richardson, C. A., & McNamee, M. G. (1984) *Biochemistry 23*, 2329–2338.
Weber, M., & Changeux, J. P. (1974) *Mol. Pharmacol. 10*, 1–140.
Wennogle, L. (1986) *Handb. Exp. Pharmacol. 79*, 17–56.
Wilson, P. T., Gershoni, J. M., Hawrot, E., & Lentz, T. L. (1984) *Proc. Natl. Acad. Sci. U.S.A. 81*, 2553–2557.
Wilson, P. T., Lentz, T. L., & Hawrot, E. (1985) *Proc. Natl. Acad. Sci. U.S.A. 82*, 8790–8794.

Dynamic Properties of Gramicidin A in Phospholipid Membranes†

Peter M. Macdonald and Joachim Seelig*
Department of Biophysical Chemistry, Biocenter of the University of Basel, Klingelbergstrasse 70, CH-4056 Basel, Switzerland
Received June 30, 1987; Revised Manuscript Received October 5, 1987

ABSTRACT: The flexibility of the tryptophan side chains of gramicidin A and the rotational diffusion of the peptide in methanolic solution and in three membrane systems were studied with deuterium nuclear magnetic resonance (NMR). Gramicidin A was selectively deuteriated at the aromatic ring systems of its four tryptophan side chains. In methanolic solution, the tryptophan residues remained immobile and served as a probe for the overall rotation of the peptide. The experimentally determined rotational correlation time of $\tau_c = 0.6 \times 10^{-9}$ s was consistent with the formation of gramicidin A dimers. For gramicidin A incorporated into bilayer membranes, quite different results were obtained depending on the chemical and physical nature of the lipids employed. When mixed with 1-palmitoyl-*sn*-glycero-3-phosphocholine (LPPC) at a stoichiometric lipid:peptide ratio of 4:1, gramicidin A induced the formation of stable bilayer membranes in which the lipids were highly fluid. In contrast, the gramicidin A molecules of this membrane remained completely static over a large temperature interval, suggesting strong protein–protein interactions. The peptide molecules appeared to form a rigid two-dimensional lattice in which the interstitial spaces were filled with fluidlike lipids. When gramicidin A was incorporated into bilayers of 1,2-dioleoyl-*sn*-glycero-3-phosphocholine or 1,2-dimyristoyl-*sn*-glycero-3-phosphocholine (DMPC) above the lipid phase transition, the deuterium NMR spectra were motionally narrowed, indicating large-amplitude rotational fluctuations. From the measurement of the quadrupole echo relaxation time, a rotational correlation time of 2×10^{-7} s was estimated, leading to a membrane viscosity of 1–2 P if the rotational unit was assumed to be a gramicidin A dimer. For DMPC in the gel state, we observed an immobilization of the peptide molecules. The tryptophan side chains of the immobilized gramicidin A in both the DMPC membrane in the gel state and the stoichiometric gramicidin A–LPPC membrane were found to execute rapid fluctuations of small angular amplitude with correlation times $\tau_c < 10^{-8}$ s.

The functioning of membrane proteins can be influenced by the physical properties of membrane lipids [for a recent review, see McElhaney (1982)]. However, it is not yet clear just which structural features of a given protein are sensitive to lipid properties and can translate into functional changes.

^{2}H nuclear magnetic resonance (NMR)[1] offers several unique advantages for characterizing molecular structure and dynamics in membrane proteins, and a number of such studies

† Supported by Swiss National Science Foundation Grant 3.521.86. P.M.M. was a recipient of a Medical Research Council of Canada postdoctoral fellowship.

[1] Abbreviations: NMR, nuclear magnetic resonance; GA, gramicidin A; LPPC, 1-palmitoyl-*sn*-glycero-3-phosphocholine; DMPC, 1,2-dimyristoyl-*sn*-glycero-3-phosphocholine; DOPC, 1,2-dioleoyl-*sn*-glycero-3-phosphocholine; Tris-HCl, tris(hydroxymethyl)aminomethane hydrochloride.

0006-2960/88/0427-2357$01.50/0